NON DETERMINISTIC ANALYSIS OF A SCRAMJET PROPULSION SYSTEM

Schütte, G., Staudacher, S.
Institute of Aircraft Propulsion Systems
Pfaffenwaldring 6
Stuttgart

OVERVIEW

The design of hypersonic propulsion systems is characterized by strong, non-linear interactions and high sensitivity to small variations. Usual deterministic methods like mean line calculations based on CFD or empirical studies are of limited suitability to answer the question of robust design and imply the need of a probabilistic approach to evaluate the sensitivity of system performance.

Especially the hypersonic environment is filled with uncertainty. On one hand even high fidelity numerical simulations of hypersonic flow necessarily include several simplifications such as turbulence models or grid imperfection, credible experimental data to validate those simulations is sparse. On the other hand the precise forecast of the environmental input for the simulation such as flight Mach number or altitude is hampered by the error of measurement in the hypersonic regime. As a consequence the designer has to make decisions based on uncertain knowledge. [1] [2]

To address this problem a paradigm shift is conceivable from the deterministic, single-value solutions to probabilistic density function-based solutions, which are able to take into account the effects of uncertainty. The usual approach provides the application of fidelity-reduced meta models, that try to approximate the real physics by regression of a high fidelity model. [3] [4] As a general rule these response surface (RSM) or kriging models do not represent the physics itself but a mostly linear regression of a limited number of numerical analyses or experimental data. The great advantage of response surface methods is, that the result can be computed within a few seconds and that the regression functions use to be sufficiently smooth, what makes them in particular suitable for gradient based optimisation methods. But especially this can be the source of significant error, because the target function in hypersonic regimes uses not to be continuously differentiable. The design space has to be simply connected; otherwise the linearized meta model feigns the existence of a solution, that is located in an unfeasible region of the design space even if it might be surrounded by feasible solutions. For an efficient use of these models a close knowledge of the design space's shape is necessary, what can not be granted during preliminary design phase. Following this argumentation, a modular, low fidelity approach for preliminary scramjet design is presented in this paper, which combines sufficiently high speed computation for probabilistic analysis with a direct depiction of dominating physical phenomena. Emphasis was put on the model in principle and the qualitative behaviour of the scramjet combustor regarding ignition and thermal choke due to small environmental fluctuations in combination with the inherent model uncertainty.

SYMBOLS AND NOTATIONS

Variables

T	Temperature [K]
Ma	Mach number [-]
ρ	Density [kg/m³]
p	Pressure [bar]
$p(x)$	Probability of x [-]
ε	Error parameter [-]
η	Efficiency [-]
σ	Standard deviation [-]
μ	Mean value [-]
$\dot{m}$	Mass flow [kg/sec]
AoA	Angle of attack [°]

Subscripts

0	Free stream
31	Combustor entrance
4,7	Combustor exit
MIX	Mixing
t	Total

Abbreviations

PDF	Probability density function
MCS	Monte Carlo simulation
RLV	Reusable launch vehicle
RSM	Response surface method
ER	Equivalence ratio
ISP	Specific impulse

1. DETERMINISTIC MODEL

The first step towards any probabilistic analysis consists in the definition of a deterministic computational model that provides the performance data of the scramjet engine in suitable accuracy. To improve accuracy and manageability of the model, a modular approach is recommended. In modern software architectures the modelling technique and numerical methods applied to the engine modules can be diverse. The modules and depicted notation of the flow planes for the deterministic model are shown in FIG. 1.

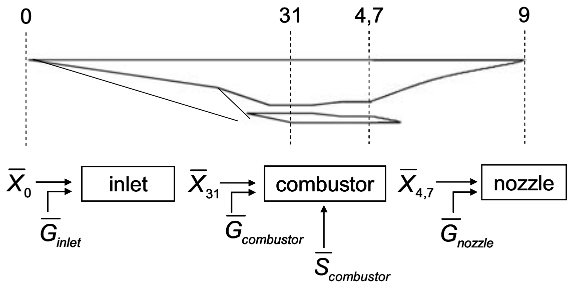

FIG 1. nomenclature of the deterministic model

The vector $\overline{X}$ denotes the flow conditions which are transferred between the engine modules at the defined interface planes. The vector $\overline{G}$ contains the geometric parameters such as ramp angles or segment lengths. The vector $\overline{S}$ contains operating parameters of the modules such as the equivalence ratio, fuel temperature and mixing efficiency.

1.1. Inlet

The function of the inlet consists in the compression of the caught air mass flow by an oblique shock system, so one of the central requirements of the inlet model is to reproduce the correct shock position. This is achieved by a 2D Euler computation of the inlet. A discontinuous Galerkin finite element scheme is used to solve the compressible Navier Stokes equations in 2D on an unstructured mesh using h/p adaptivity. FIG 2 shows the Mach number distribution of the inlet. For a detailed description see [5].

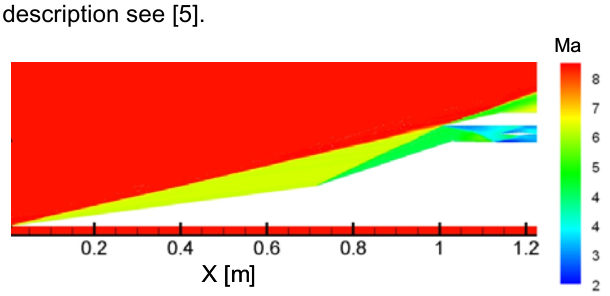

FIG 2. inlet flow field

1.2. Combustor

In the combustor the chemical reaction of the compressed air with the injected fuel takes place, hence the focus in this modelling approach lies upon fuel mixing and ignition. Furthermore, due to the high Mach number expected at the combustor entrance, chemical disequilibrium must be taken into account. As a consequence the combustor model combines a RAND-algorithm to solve a 12-species reaction scheme for non-equilibrium chemistry with a one dimensional flow computation. The local mixing of fuel and oxidizer is approximated by the exponential mixing rule, [6]

$$\eta_{MIX} = 1 - e^{\frac{\ln(1-\eta_{max})}{L_{MIX}} \cdot x} \tag{1}$$

where η_{MIX} is called the local mixing efficiency, $\eta_{\max}$ the ideal mixing efficiency after a running length L_{MIX}. In addition the model performs a simplified calculation of the turbulent boundary layer displacement thickness and the heat transfer to the combustor walls. [7]

2. PROBABILISTIC FRAMEWORK

As an extension to the deterministic model, a probabilistic analysis requires a possibility to access the systems overall robustness in dependence of the occurring uncertainty.

2.1. Extension of the Deterministic Model

In the current setup each deterministic single point value is extended by a probability density function (PDF) though multiplication with a specific error function ε_i. This function contains shape and standard deviation σ_i of the parameter, the mean value μ_i of ε_i is fixed to be unity to provide the deterministic solution in absence of uncertainty (σ_i =0). This allows the interpretation of σ_i as a kind of reliability factor. Optionally any parameter independent of its nature (conditional, operational or geometric) can be vested with this specific uncertainty. The characteristics of the used PDF's are discussed in chapter 2.2. Furthermore the data exchange in between the modules and with the design space is managed by the integrated parsing functions following the depicted setup (FIG 3.).

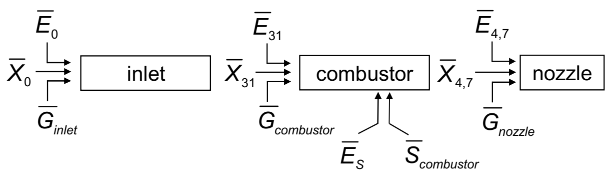

FIG 3. setup of the probabilistic system

Here $\overline{X}_i$ again represents the vector of flow properties, $\overline{G}_i$ the geometric parameters, $\overline{S}$ the operating parameters and $\overline{E}_i$ the vector of the specific uncertainties ε_i.

2.2. Accessing Uncertainty

In accordance with [8], two different kinds of uncertainty must be distinguished, whose attributes must be treated in different manner. The first one arises from the fact, that any input parameter to a numerical model like geometry, flight condition and operating point has and underlying uncertainty with regards to the achieved real value. As a general rule parameters of that kind are found in extremely complex systems, where an unmanageable large number of parameter influence each other in a mostly unknown way (“butterfly effect”, [9]) This uncertainty called “adhesive uncertainty“ in the following.

The other type of uncertainty arises from the concept of the incapability of engineering models to describe a physical process exactly and in every detail. Every model is affected with a certain error due to assumed simplification or negligence. Hence this kind of uncertainty is a part of the model itself it is named “inherent uncertainty“. Examples and further information are given in [10].

2.2.1. Adhesive Uncertainty

Adhesive Uncertainty is owing to natural scattering of parameters and is also called “aleatory uncertainty“. [11] It basically expresses the variability of input design variables: In the preliminary design phase the inlet inflow conditions are derived from the U.S. standard atmosphere at the assumed design altitude. The standard atmosphere is a useful reference to compare performance at standardized flight conditions, nevertheless the flight conditions during a real flight might deviate from the standard values. A measure for the size of those possible deviations is given in FIG 4.

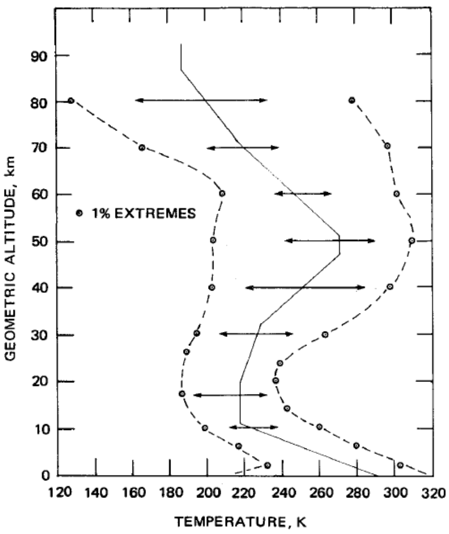

FIG 4. Variation relative to the U.S standard atmosphere [12]

Likewise Mach number, angle of attack or fuel mass flow are affected by a specific measurement uncertainty, while the systems geometry is subject to fabrication tolerance.

2.2.2. Inherent Uncertainty

Part of the inherent uncertainty occurs due to the underlying numerical imperfection, e.g. truncation errors, dependencies on mesh quality and time step size.

2.3. Assessment of the Uncertainty

The individual uncertainties have to be assessed and put into the mathematical form described in 2.1 in order to feed the probabilistic evaluation. Two different considerations have been made in the presented investigation, i.e. the Laplaces’s Principle [13] and the Moivre-Laplace central limit theorem. [14]

The inherent mesh and step size sensitivity defines the upper and lower limit of an interval, where the “real” solution of the applied numerical method will be located in. It can be assumed, that with an increasing mesh refinement the solution converges to the “real” inviscid solution, but for the purpose of reduction of computing time, a more coarse mesh is applied here. As there is no further information about the solution, laplaces’s principle of insufficient reason indicates treatment of inherent uncertainties as uniform distributed uncertainties like

(2) $$p(x) = \begin{cases} \dfrac{1}{h-l} & \text{for} \quad l \le x \le h \\ 0 & \text{else} \end{cases},$$

where h denotes the highest possible value and l the lowest.

A different consideration has been made for the adhesive uncertainty, which affects parameters like free stream temperature or flight Mach number as well as fabrication caused variances in engines geometry. Those are subjected to a long chain of dependencies, each link affected with a certain probability. Hence the convolution integral

$$p\ (x) = p_1(x) \cdot p_2(x) \cdot p_3(x) \ldots$$

converges against the normal distribution disregarding the shapes of the initial distributions $p_i(x)$.

(3) $$\xrightarrow{i \to \infty} p\ (x) = \frac{1}{\sqrt{2\pi\sigma}} e^{-\left(\frac{(x-\mu)^2}{2\sigma^2}\right)}$$

This fact is known as the Moivre-Laplace central limit theorem and justifies the assumption of a normal shaped PDF for those variables.

2.4. Quantification of the Uncertainty

After defining the different types of uncertainty and the resulting PDF type, the standard deviation of the particular uncertainty factor ε_i needs to be defined. This is accomplished under the "± 3 – sigma" postulate, which means, that 99.73 % of the occurring values for the parameter lie within the interval between the highest and the lowest possible value. The uncertainty factors ε_i assume the following shape: $\varepsilon_i = f(\mu, \overline{\sigma})$ with

(4) $\mu \equiv 1$,

(5) $$\overline{\sigma} = \frac{\sigma}{l + \frac{h-l}{2}} = \frac{\frac{1}{6} \cdot (h-l)}{l + \frac{h-l}{2}}$$

and

(6) $$\overline{\sigma} = \frac{1}{l + \frac{h-l}{2}} \cdot \sqrt{\frac{(h-l)^2 - 1}{12}}$$

for a Gaussian (Eqn. 5) and for a uniform (Eqn. 6) distribution, where h stands fort he highest possible and l fort he lowest possible value. In this context it is of utter importance, that the error quantifications used in the probabilistic model are to be determined in cases and conditions that are physically similar to the considered ones, because in most cases it can not be excluded, that the error itself is a function of the surrounding conditions.

As it is visible in FIG 4, the difference between the measured data and the modelled values of the standard atmosphere varies with the altitude. In the presented case for the aspired altitude of 30km a variation between 206.3K and 246.1K for the free stream static temperature is expected. The same data is used to access the adhesive uncertainty of the free stream density and the static pressure. Assuming an industrial standard measurement method for the true air speed and the angle of attack, the specific uncertainty of flight Mach number and angle of attack are derived from the corresponding data sheet. [15]

One of the central features of the presented scramjet configuration is the horizontal injector strut with the lobed trailing edge. (FIG 5.)

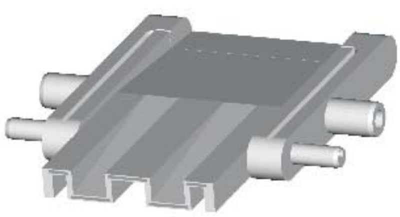

FIG 5. Central injector strut

The ignition behaviour of the combustor is heavily influenced by the above injector strut design through an improved mixing efficiency η_{MIX}. The local value of the mixing efficiency is calculated via Eqn. (1) and hence is dependant on the mixing length L_{MIX} and the maximum mixing efficiency η_{MAX}. High fidelity 3D numerical investigations of the mixing behaviour have been consulted [16] in order to derive L_{MIX} and η_{MAX} with the associated uncertainties. FIG. 6 illustrates the mixing efficiency in dependence of the mixing length. It becomes obvious that the exponential mixing rule fits the high fidelity computations well for high mixing lengths if $\eta_{max} = 0.967$ and mixing length L_{MIX} of 0.35 are chosen.

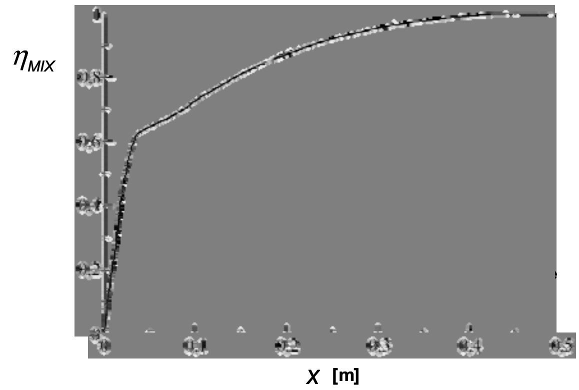

FIG 6. mixing capacities of the lobed injector strut

The evaluation of the exponential mixing rule at the maximum mixing length of 0.35m and a comparison of the assumed maximum mixing efficiency lead to a standard deviation of $\sigma(\varepsilon_{\eta_{mix}}) = 0.0077$.

The usual approach for fuel mass flow measurement is to compute the mass flow form the measured volume flow, - here a variance of +/- 1% - is obtained from a corresponding data sheet. [17] The static fuel temperature has been calculated based on experimental results and a simplified one dimensional calculation for the heat transfer to the fuel flow in the strut. A mean static fuel exit temperature of 409 K has been obtained. A standard deviation of ± 27.17 K has been derived taking into account the temperature variations which have been observed in the underlying experiment.

The numerical variance of the inlet calculation is dependant on mesh and step size resulting in a uniform distributed error. A Mach 8 flow over a 2D wedge with a deflection angle similar to those appearing in the inlet (FIG 7.) has been used to estimate the standard variation of the inherent uncertainty of the intake calculation. For the chosen 2D Euler approach this uncertainty mainly consists in the number of cells used for the shock capturing.

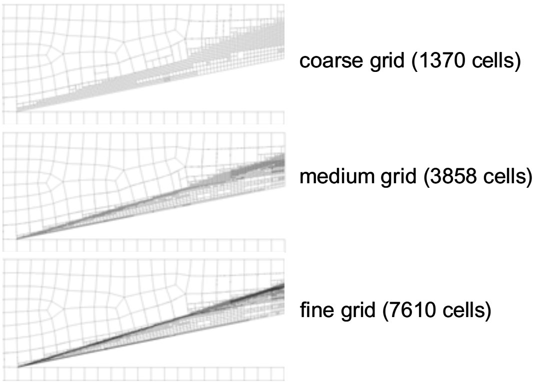

FIG 7. different meshes for the 2D wedge

The obtained averaged static pressure in the outflow plane of the 2D wedge is shown in FIG 8 as a function of number of mesh nodes. A model function of the form $y = a \cdot x^b + c$ has been fitted to the results. The expected value of the static pressure has been derived from exploiting the model function for $x \to \infty$. The standard deviation has been derived at the point of 4000 nodes under the assumption of a purely statistical remaining error.

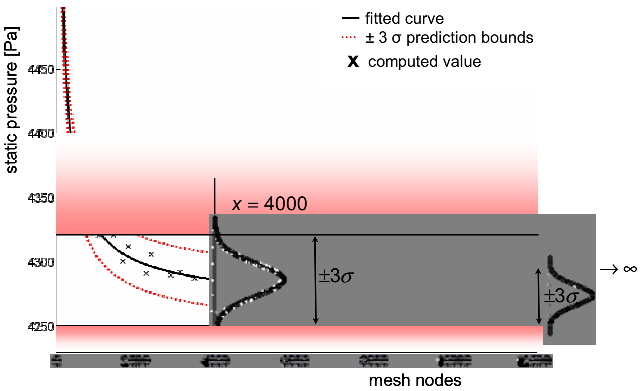

FIG 8. distribution of static pressure in dependence of mesh accuracy

Using a similar approach for the other flow conditions, the derived error-vector assumes the following values:

$$\overline{E}_{31,inherent} = \begin{pmatrix} \varepsilon_p \\ \varepsilon_T \\ \varepsilon_{Ma} \end{pmatrix}_{31} = \begin{pmatrix} \varepsilon_p : \mu = 1, \overline{\sigma} = 0.0047009 \\ \varepsilon_T : \mu = 1, \overline{\sigma} = 0.0016684 \\ \varepsilon_{Ma} : \mu = 1, \overline{\sigma} = 0.0028815 \end{pmatrix}_{31}$$

2.5. Methodology

To cover all possible combinations of design parameters a full factorial study is needed, accounting for N^n simulation runs, where N stands for the number of levels considered and n for the number of parameters taken into account. That means in facts that a full factorial study of 10 parameters at 3 levels for each parameter (for example mean value, +/- 1%) requires 59049 simulation runs. In combination with execution times of about 10 minutes the required time of 1.234 years clarifies the main challenge of probabilistic methods. As a consequence it is obvious, that the execution of the probabilistic investigation has to be optimized. Due to the fact, that a complex system like a scramjet engine is described by a plenitude of design parameters, in the forefront of the analysis a decision, which parameters are important to be taken into account, has to be reached. A preliminary pareto analysis can be of used for this decision. The reduction of the levels, where the particular parameter is evaluated, has to be avoided as far as possible, because the behaviour of the scramjet is expected to be highly non-linear and the predicted performance would become more erroneous.

The most effective way to reduce the required number of simulation runs without significant loss in accuracy is the use of descriptive sampling methods. Usual Monte Carlo methods employ a simple random sampling, where all sample points are distributed randomly over the design space (FIG 9, left). In the presented study the descriptive latin hypercube sampling was employed (FIG 9, right). For the use of this method the n-dimensional design space hyperplane is subdivided into m equally probable intervals defining a square grid. Every row and every column is only sampled once, so a more homogenous sampling is achieved.

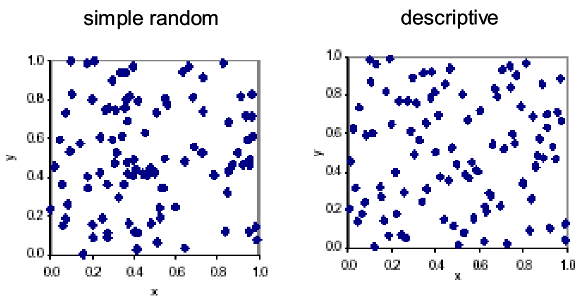

FIG 9. comparison of sampling methods

The depicted example in FIG 10 shows the distribution of 250 runs of a normal distributed variable, μ=1 and σ=0.1, with a simple random (right) and a descriptive sampling method (left)

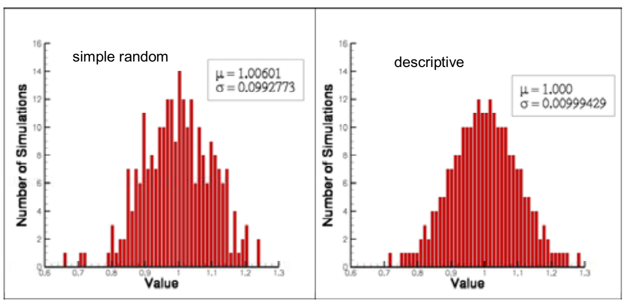

FIG 10. quality of sampling methods

In the light of its higher uniformity, the descriptive sampling can be regarded as the more suitable method, because less simulation runs are required to sample the whole design space with a higher accuracy.

3. ENGINE CONFIGURATIONS

The GRK 1095/1 scramjet project [18] was chosen as baseline configuration. This configuration consists of a 2D external compression inlet with ramp angles of 7.5 and 18.4 degrees respectively to obtain a contraction ratio of 6.5 and a horizontal cowl. The leading edges of the first ramp and the cowl are in this context regarded to be sharp such as the leading edge of the injector strut.

Two combustor designs have been investigated to demonstrate usefulness of the applied methods with regards to the robustness of the combustor designs. The shape of combustor design No. 1 is defined by a total length of 0.8 m, subdivided in three segments of 0.2, 0.2, and 0.4 m and divergences of 0.0, 1.5 and 3.0 degrees, respectively. The geometry of the modified combustor design No. 2 is defined by segment lengths of 0.3, 0.2 and 0.3 m and divergence angles of 0.0, 1.0 and 2.0 degrees respectively.

	upper limit	lower limit	deterministic value (predicted by ISA model)	standard deviation
ρ [kg/m³]	0.0212	0.0148	0.018012	0.0005272
T [K]	246.1	206.3	226.65	6.633
Speed of sound [m/sec]	275.8	328.9	302.36	8.8487

TAB 1. free stream conditions

The investigation was carried out at a reference point which is defined by a flight Mach number of 8 in 30km altitude. In combination with the systematic uncertainty of the U.S. standard atmosphere this results in the following set of free stream input variables with an assumed Gaussian distribution. (TAB 1) The basic design parameters with the according noise parameter that represents the variables probabilistic distribution are documented in TAB 2.

	deterministic value	$\varepsilon_{i,j}$		
		type	mean	standard deviation
ρ_0 [kg/m³]	0.018012	normal	1	0.001757
T_0 [K]	226.65	normal	1	0.0313994
Ma_0	8	normal	1	0.0045432
AoA [°]	0	normal	0	+/-1°
ER	1	normal	1	0.00333
T_B [K]	450	normal	1	0.037037
η_{MIX}	0.967	normal	1	0.0079628
Ma_{31}	-	uniform	1	0.0167681
T_{31} [K]	-	uniform	1	0.0167681
$\dot{m}_{31}$ [kg/sec]	-	uniform	1	0.0167681

TAB 2. scramjet design parameters

All geometric parameters of the engine are assumed to be deterministic.

3.1. Data Propagation

According to the terminology introduced in 2.1 the parameters are merged to vectors corresponding to their type and shape. The internal treatment of the data flow vectors is described by

$$\tilde{X}_0 = \overline{X}_0 \cdot \overline{E}_0 = \begin{pmatrix} \rho_0 \\ Ma_0 \cdot \cos(AoA) \\ Ma_0 \cdot \sin(AoA) \\ T_0 \end{pmatrix} \cdot \begin{pmatrix} \varepsilon_{\rho_0} \\ \varepsilon_{Ma_{x,0}} \\ \varepsilon_{Ma_{y,0}} \\ \varepsilon_{T_0} \end{pmatrix}, \tag{6}$$

where $\overline{X}_0$ stands for the deterministic free stream conditions derived from the U.S. standard atmosphere and $\varepsilon_{i,0}$ representing it's reliability. The treatment of the combustor entrance data is handled in a similar way.

$$\tilde{X}_{31} = \overline{X}_{31} \cdot \overline{E}_{31} = \begin{pmatrix} p_{stat,31} \\ T_{stat,31} \\ Ma_{31} \\ ER \\ T_{Fuel} \\ \eta_{MIX} \end{pmatrix} \cdot \begin{pmatrix} \varepsilon_{p_{31}} \\ \varepsilon_{T_{31}} \\ \varepsilon_{Ma_{31}} \\ \varepsilon_{ER} \\ \varepsilon_{T_{Fuel}} \\ \varepsilon_{\eta_{MIX}} \end{pmatrix}, \tag{7}$$

where the Vector $\overline{X}_{31}$ depicts the computed outflow from the inlet module and the operational parameters of the combustor module, $\overline{E}_{31}$ representing the model error consisting the specific errors $\varepsilon_{i,31}$ derived from the numerical variance analysis such as the adhesive uncertainty ε_j of the operational parameters.

4. RESULTS

A study of the qualitative behaviour of the scramjet combustor regarding ignition and thermal choke has been carried out using the methods described above. In a first step, the described two combustor geometries where studied by 1000 simulation runs each. The combustor inlet flow conditions have been simulated taking into account the inherent uncertainty $\overline{E}_{31}$ assuming constant flight conditions.

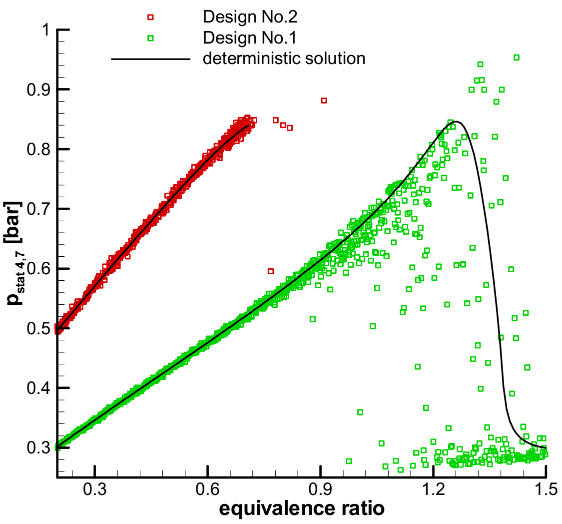

FIG 11. static pressure in the combustor exit plane

In FIG 11 it becomes obvious that geometry No. 2 leading to higher combustor exit pressures holds the risk of thermal choking already at equivalence ratios smaller than 0,7. The obtainable equivalence ratio is lower for the slender combustor No. 2, because the chemical heat release causes a sharper increase in temperature and a concurrent drop of the Mach number.

With increasing equivalence ratios a consistent increase in combustor exit pressure is observed, which reaches its maximum at an equivalence ratio of 1.25. The subsequent sharp decrease is a result from higher fuel mass flow. The delayed ignition provokes, that the reaction zone is blown out of the combustor so no pressure rise inside the combustor is recognizable. Although the inherent uncertainty as well as the deterministic solution for the inlet flow is identical for both MCS, the variance of the static pressure with respect to the deterministic solution is greater for the combustor design No. 1 and extremely increases with the equivalence ratio.

A closer look at the outliers for the modified configuration yields to the conclusion, that for these points no stable combustion can be assumed. For the baseline configuration these outliers are defined by high equivalence ratios and low static pressures. Delayed ignition is the reason for this phenomenon which is supported the low combustion efficiencies about 1-3% which is observed for these points.

The thermal choking of combustor geometry No 2 leads to the discontinuity in specific impulse which is shown in FIG 12. Also with respect to specific impulse geometry No. 1 behaves better tempered. Again it can be obtained, that the variance is larger for the baseline geometry, especially at high equivalence ratios, where ignition delay or flame quenching lead to a less abrupt decrease in the specific impulse, can be observed. The outliers in FIG 12 are the same as in FIG 11.

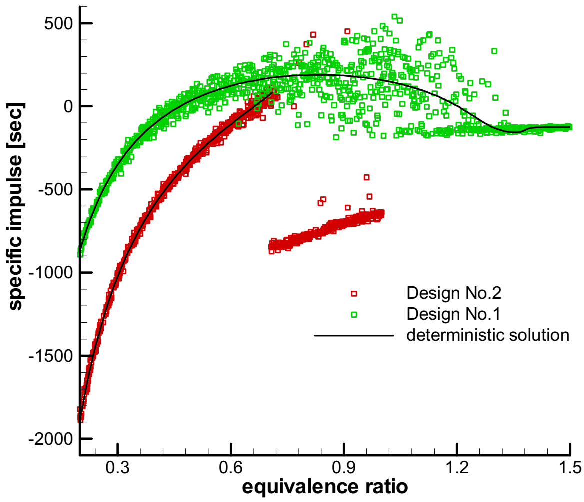

FIG 12. specific impulse for the two combustor geometries

The increased risk of thermal choking for the combustor geometry No. 2 is documented in FIG 13 by plotting the frequency of simulations leading to combustor choking as a function of the position of the normal shock (choking length) in the combustor.

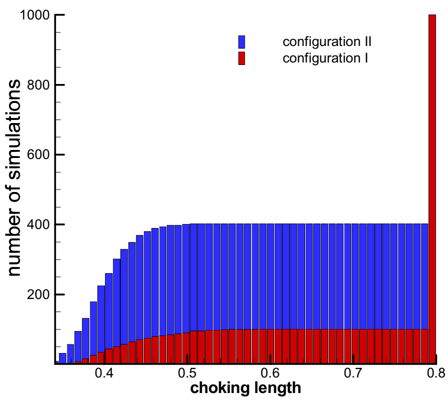

FIG 13. risk of thermal choking

Following the above discussion, configuration No. 1 is retained for analysis of the system taking into account variations in the flight condition. Its higher robustness towards thermal choking is assumed to be the crucial factor, although a larger variance of the output values is expected.

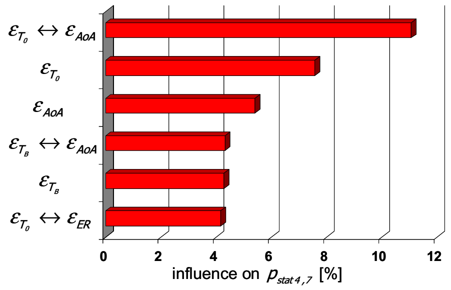

FIG 14. pareto plot $p_{stat4,7}$

In FIG 14 the pareto plot of the static pressure in the combustor outflow plane for the probabilistic system analysis is depicted, wherein the six most important parameters are identified. It can be discovered, that not only individual parameters such as ε_{T_0} or ε_{AoA} are responsible for the variance of $p_{stat4,7}$, but also interactions of them like $\varepsilon_{T_0} \leftrightarrow \varepsilon_{AoA}$. The influence of a distinct inherent uncertainty ε_{ER} is about 4% in combination with a high uncertainty in the free stream Temperature T_0, while the influence of the error ε_{ER} itself is less than 0.1%. The influence of the not depicted parameters is lower than 4%.

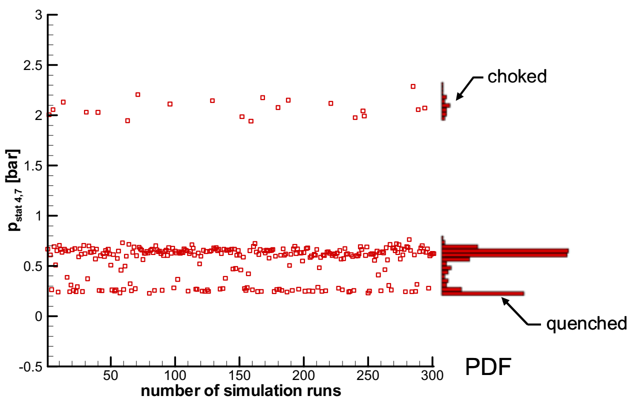

FIG 15. anthill plot and resulting PDF for $p_{stat4,7}$

As can be seen in the PDF for $p_{stat4,7}$ (FIG 15.) there are 3 peaks occurring representing 3 different operational conditions of the combustor. The most probable condition is a normal operating combustor characterized by a mean value of about 0.65bar. The two other conditions represent a choked combustor (top) and a quenched combustor where no ignition takes place (bottom).

Resuming FIG 14, where the free stream temperatures uncertainty was identified as one of the authoritative parameters for $p_{stat4,7}$, FIG 16 relates the combustor condition to the variations indicated by the U.S standard atmosphere. If the variance is sufficiently small, the static pressure slightly increases with estimated lower ambient temperatures.

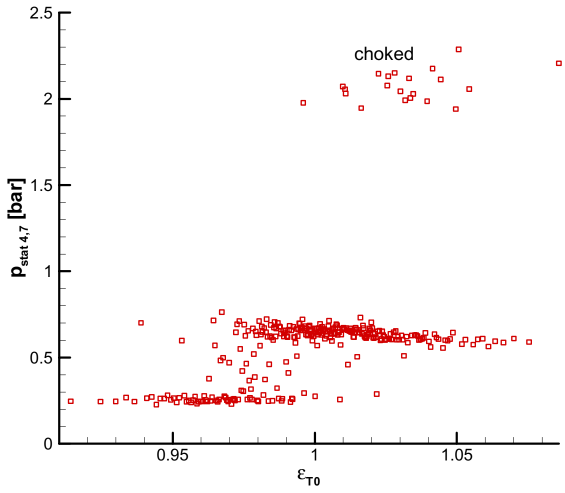

FIG 16. trend in $p_{stat4,7}$ versus ambient temperature variation

For higher variances the combustor fails due to thermal choke in case of increasing ambient temperature and due to flame quenching for opposite variances. The obtained results for the ISP show a similar behaviour.

To access the phenomenon of interactions the dependence of the static pressure $p_{stat4,7}$ on the mass flow in the combustor entrance is considered. (FIG 17.)

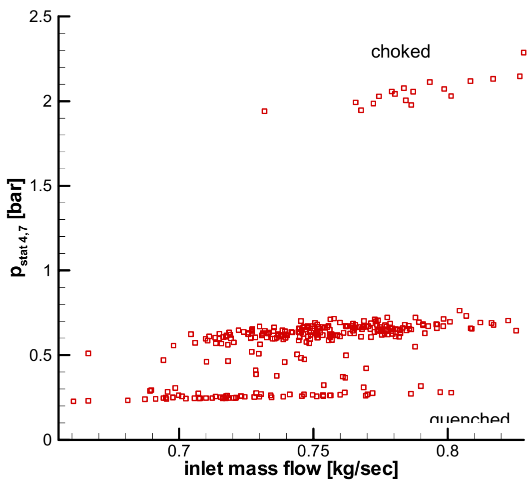

FIG 17. trends of $p_{stat4,7}$ versus mass flow

Similar to FIG 16, a dependency of the combustors operational behaviour on the mass flow is ascertainable. High intake exit mass flows lead to an increased risk with regards to thermal chocking. The pareto plot for the intake exit mass flow (FIG 18.) identifies the ambient density error ε_{ρ_0} and the error in the angle of attack ε_{AoA} as two of the most important parameters. In this case the not mentioned parameters have an influence of less than 1.5% what leads to the conclusion that the inlet mass flow is dominated by the depicted variables.

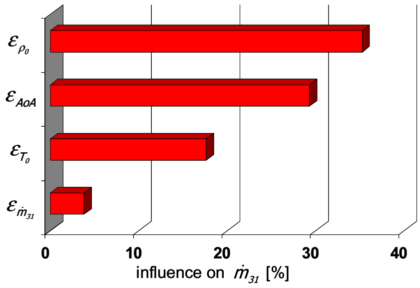

FIG 18. pareto plot for the inlet mass flow

5. SUMMARY

A non-deterministic analysis of a parameterized scramjet engine by using a modular, fast computing low fidelity approach has been presented, that does without employment of linearized meta models. The model combines 2D and 1D methods as well as non-equilibrium chemistry and is regarded as affected with inherent uncertainty due to model imperfection as well as adhesive uncertainty due to measurement and control errors. The discussed results of the Monte Carlo simulations suggest a high sensitivity of the actual baseline geometry of the scramjet propulsion system with regards to the expected uncertainties and the significant impact of uncertainties interaction.

6. ACKNOWLEDGEMENTS

This research is part of the research programme of the GRK 1095/1 and mainly supported by the Deutsche Forschungsgesellschaft (DFG).

REFERENCES

[1] Bandte, O.: "*A Probabilistic Multi-Criteria Decision Making Technique for Conceptual and Preliminary Aerospace Systems Design*", Dissertation, Georgia Institute of Technology, 2002.

[2] Mavris, D. N.; DeLaurentis, D. A.; Bandte, O.; Hale, M. A.: "*A Stochastic Approach to Multi-disciplinary Aircraft Analysis and Design*", 36th Aerospace Sciences Meeting & Exhibit, January 12-15 1998, Reno, NV

[3] Daberkow, D.D.: "*A Formulation of Metamodel Implementation Processes for Complex System Design*", Dissertation, Georgia Institute of Technology, 2002.

[4] DeLaurentis, D.A.; Mavris D.N.: "*Uncertainty Modelling and Management in Multidisciplinary Analysis and Synthesis*", AIAA Journal, Vol. 33, No. 2, February 1995, pp.246-251.

[5] Gassner, G.; Lörcher, F.; Munz, C.-D.: "*A contribution to the construction of diffusion fluxes for finite volume and discontinuous Galerkin schemes*", Journal of Computational Physics 224, 2007 pp 1049–1063.

[6] Murthy, S.N.B.: "*Basic Performance Assessment of Scram Combustors*", in: Curran, E.T., Murthy, S.N.B.: "*Scramjet Propulsion*", Progress in Astronautics and Aeronautics, Vol. 189, 2000.

[7] Scheuermann, T., von Wolfersdorf, J.: "*Eindimensionale Modellierung von thermodynamischen Vorgängen bei der Überschallverbrennung*", Diploma Thesis, Institut für Thermodynamik in der Luft- und Raumfahrt, Stuttgart University, 2005.

[8] Ferson, S.; Ginzburg, L. R.: "*Different methods are needed to propagate ignorance and variability*", Reliability Engineering and System Safety 54, 1996, pp 133-144.

[9] Lorenz, E. N.: *"Deterministic Nonperiodic Flow",* Journal of the Atmospheric Sciences, Vol. 20, 1963.

[10] Mozumder, C.K.: "*Characterization of Model Fidelity Uncertainty for Robust Design*", Master Thesis, Indian Institute of Technology Bombay, July 2005.

[11] Stamelatos, M.: "*Probabilistic Risk Assessment Procedures Guide for NASA Managers and Practioners",* Office of Safety and Mission Assurance, NASA Headquarters, Washington, 2002.

[12] National Aeronautics and Space Administration: "*U.S. Standard Atmosphere",* 1976.

[13] Sinn, H. W.: "*A Rehabilitation of the Principle of Insufficient Reason"*, The Quarterly Journal of Economics, 1980

[14] Fahrmeir, L.; Künstler, R.: Pigeot, I. Tutz, G.: "*Statistik. Der Weg zur Datenanalyse*", Springer Lehrbuch, 4. Aufl. 2003

[15] SpaceAge Control, Inc., data sheet of the straight-nose air data boom 100600, http://www.spaceagecontrol.com/100600.pdf

[16] Jellinghaus, K.; Gerlinger, P.; Aigner, M.: "*Numerical Investigation of Mixing Enhancement by Lobed Strut Injectors in Turbulent Reactive Flow*" 18th International Sysmposium on Airbreathing Engines September 2-7. 2007 Beijing, Cina

[17] Schaefer Technoligie GmbH, data sheet of massflow gauge Hasting HFM-300/HFC-302, http://www.schaefer-tec.com/GER/GP04002.HTM

[18] Gaisbauer, U.; Weigand, B.; Reinartz, B.; Kau, H.P.; Schröder, W.: Research training group GRK 1095/1: "*Aero-Thermodynamic Design of a Scramjet propulsion system*", 18th International Sysmposium on Airbreathing Engines September 2-7. 2007 Beijing, Cina